Chapter 2
Experiment

Total PFNS is formed due to contributions of different sources of neutrons. We still assume that some part of neutrons is emitted due to unknown mechanism. Another part (we still assume that this is the main part) is emitted from accelerated fission fragment (FF), and energy-angular distributions of prompt fission neutron (PFN) depend very much on the direction between FF and neutron detector (ND), and particular properties of FF like masses, total kinetic energy (TKE), and so on. Due to complicate nature of neutron emission in fission, sometimes unknown, the prompt fission neutron spectrum (PFNS) measured in particular experiment may be destroyed very much.

Fission events should be selected to avoid background counting. The best way is detecting of FF as a unique signature of fission events. This experiment may be organized in different ways.

The first type of experiment, all FF emitted from fissile material, is counting in special detector. This detector should be constructed in such a way to avoid fragment losses. Let us name this type as "total FF integrated experiment."

The experiment may be organized in such a way ("differential FF experiment") to investigate energy-angular distribution of neutrons relative to fixed FF with particular properties and direction relative to ND. This type is very important for investigation of neutron emission mechanism, but results of this may be used also to estimate the total PFNS as integral of above-mentioned experimental data. The problems connected with this procedure may destroy result and should be discussed in each particular experiment. The main criteria that the procedure is self-consistence, is the agreement of PFNS measured with this second type of experiments with total PFNS result (first experiments).

The PFNS has broad energy distribution. So any neutron spectrometer operating with input energy E_0 may be used for measurement of PFNS for energy interval $E > E_0$. Let us name this experiment as "solid sample" (third type).

All experiments have got particular advantages and disadvantages:

- First experiment can be easily used at thermal point where neutron flux and fission cross section are high. At input energy >1 MeV, a large amount of fissile material should be loaded in FF detector. This factor may give strong influence on final result.

- Second experiment is unique for investigation of neutron emission mechanism, but may destroy PFNS due to numerical integration procedure.
- Third experiment is very useful for $E_0 = 0.5$ MeV where intensive neutron source ^{7}Li(p,n) is available. An additional correction for time spread over fissile sample should be done. However, there is very big data spread for ^{235}U PFNS measured with this method. The nature of this problem is unknown. For higher input energies, experimental data cover limited energy range $E > E_0$, which complicates data analysis and evaluation.

Different techniques were used for PFNS investigations. Since the review [36] prepared in 1976, practically nothing changed. In a number of works, the method of registration of recoil protons [35], and ^{3}He(n,p) [36] and ^{6}Li(n, α) [10] reactions' products were used.

Time-of-flight (TOF) method is used now practically in all experiments as the most accurate one. NDs are also the same types: on the basis of ^{6}Li(n,α) reaction—lithium glasses, ^{6}LiI(Eu) crystal, and ^{235}U(n,f) in ionization chamber (IC) for energy range <3 MeV, and hydrogen organic scintillator with neutron gamma-ray discrimination for fission neutron energy >0.5 MeV, with detail investigation of the ND efficiency.

The traditional method:—yield of mono-energetic neutrons from ^{7}Li(p,n), D(d,n), T(p,n), reactions, and (n,p) scattering were used in many experiments' ND efficiency investigation. After estimation of the ^{252}Cf PFNS like a standard in 1986 [29], the ratio measurement became the traditional method for ND calibration.

2.1 Microscopic Experiments

As was mentioned above, TOF experiments are the most accurate ones. Therefore, only this type of microscopic experiments will be discussed here.

2.1.1 Methods of FF Counting

In [25], a ^{252}Cf fission source of intensity $\sim 1 \times 10^4$ 1/s was prepared by electrodeposition on thin tantalum foil. The diameter of layer ^{252}Cf was 7 mm. The foil with layer was placed inside a vacuum chamber made of 1-mm-thick aluminum. At a distance of 1 mm from the ^{252}Cf a semiconductor detector was placed for counting of FF. The silicon surface-barrier detector was made of material with a specific resistance of 300 om*cm and its working diameter was 20 mm. Pulses formed by FF were separated very well from α-particles events. The specific problems were rather poor time resolution ~ 4 ns and short life time of semiconductor detector. Author changed the FF detector each time when FF count rate was reduced by $\sim 1.5\%$. The integral radiation dose to each counter during the experimental run was 2.7×10^8 1/cm^2 for FFs. The total operation time of one counter was ~ 24 h.

In the pioneering work of [13], a Cf source with an initial intensity of 6.1×10^5 f/s was mounted in a gas-scintillation detector. The ^{252}CF source was electrodeposited inside a 1 cm circle onto a thin foil backing. A 100-µg gold layer covered the source to reduce the migration of Cf inside the counter. The foil was mounted at one end of a thin-walled stainless-steel scintillator tube. Good high vacuum procedures the cell prior to backfilling 28 psia with high purity xenon gas. The cell was viewed by 56UVP phototube through a quartz end window.

In the following, a similar technique was applied for counting FF rate of $1 \cdot 10^6$ f/s [38]. An additional cleaning system was used to support high light output from gas scintillator.

A larger problem of the gas scintillator for FF counting is a big amount material around the neutron source, which may destroy spectrum shape very much (see discussion in following part of this section).

The IC for FF counting is the most attractive device in comparison with the one discussed above. It can provide good time resolution, long time stability, and total amount of material around fission neutron source may be reduced as much as possible.

The IC operating in fast current mode was used as FF detector in experiments [1, 7, 19]. In these experiments, ^{252}Cf source was used for ND calibration.

In [22], Cf and U layer were placed inside the same IC. The FF count rate for U was $\sim 5 \times 10^4$ 1/s. Time resolution (IC+ND) was 1.7 ns for U section and 2.1 ns for Cf. The difference appeared due to counting of both FF for ^{235}U.

In experiments for measurement of PFNS at $E > 5$ MeV only ICs were used by all authors [2, 17, 4, 5, 32, 27]. PFNS for the ^{238}U(n,f) reaction, [17] were measured relative to those of ^{252}Cf. Time resolutions (2–3 ns) and flight paths (~ 2 m) in both sets of experiments were similar.

The particular feature of these experiments is a bid amount of fissile material, which should be placed in IC to provide reasonable run time. As a result layer thickness was high, and the efficiency of FF counting was rather low. Multilayer assembly was used (big input capacitor for preamplifier), which complicates timing fission events with good time resolution. For example, in the experiment of [2], the fission chamber efficiency was ~ 70–75% at $E_n \sim 14.3$ MeV and ~ 80–85% for $E_n \sim 6$–9 MeV [17]. In the experiments, [4, 5, 32, 27] the ^{252}Cf was incorporated into one section of the fission chamber as an admixture to the uranium layer. It allowed to reduce the influence of the fragment discrimination threshold but did not remove this effect.

In the experiments by Kornilov et al. [2, 17], the problem of stable operation "fast current preamplifier" connected to multiple layers chamber was not solved. Neutrons were detected in coincidence with fission events, but there was no timing of events. The spectra were measured in a "pulsed mode" of the accelerator. Consequently, the spectrum of "background" neutrons was time dependent and the "effect/background" ratio was poor at higher neutron energies.

The IC applied for detector calibration with ^{252}Cf in experiments [19] was operated with count rate $\sim 5 \cdot 10^4$ 1/s. The similar detector can be operated with Cf source intensity up to $\sim 3 \times 10^5$ f/s [1].

Fig. 2.1 Drawing of the ioniza-
tion chamber for the ^{252}Cf reference
source. *1* high voltage, output signal,
2 contactor, *3* ^{252}Cf layer, *4* collect-
ing electrodes, *5* insulators, *6* holder
(*thin-walled tube*), *7* gas inlet
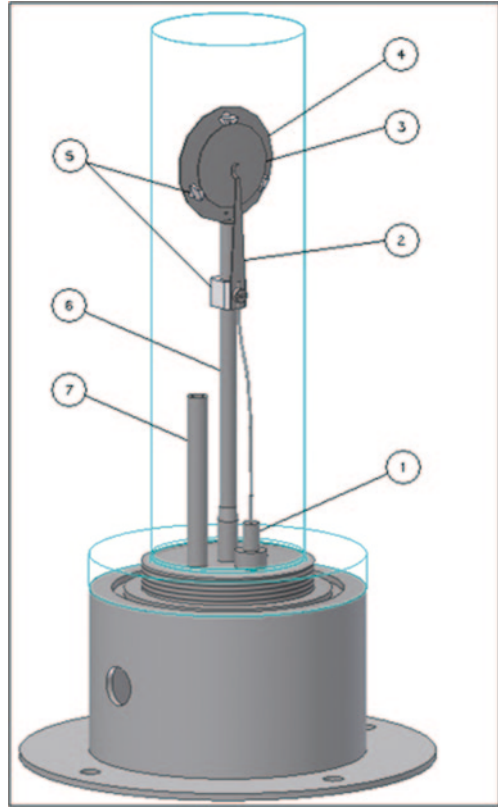
The parallel plate IC provides the current $I = en(t) \cdot v / d$, where $n(t)$—total
amount of electrons between the electrodes at the moment t, v—drift velocity of the
electrons, d—distance between electrodes. The initial amount of electrons for FFs
moving in the orthogonal direction relative to the electrodes is $n(0) = dE / dx \cdot d$. So
in first approximation, the minimal current does not depend on the distance between
the electrodes. A distance of $d = 2.5$ mm provides a rather good current ratio of 10:1
between FFs (70 MeV, Mo–Ba pair) moving along the electric field and 5.5 MeV
alpha-particles moving in a perpendicular direction. At $U = 500$ V for $Ar + 10\%CH_2$,
the drift velocity is $v \sim 5 \times 10^6$ cm/s which gives a ~ 50 ns pulse width.

A three-dimensional sketch of the ionization chamber is shown in Fig. 2.1. The
Cf layer ($\varnothing = 10$ mm) was placed on a polished stainless steel electrode ($\varnothing = 25$ mm).
The wall thickness of the chamber cover (stainless steel) was 0.2 mm. All mas-
sive parts were moved far away from the source. The chamber was filled with an
$Ar + 10\%CH_2$ mixture up to 1.2 bar. The output signal from the chamber was fed to
a fast preamplifier. Good results (stability, low noise, time resolution) were reached
with the MESYTEC charge integrated preamplifier module MPR-1—single chan-
nel charge sensitive preamplifier (QPA) with two outputs [37].

Fig. 2.2 The counting efficiency of FF for fast IC. The *arrow* shows the threshold value used
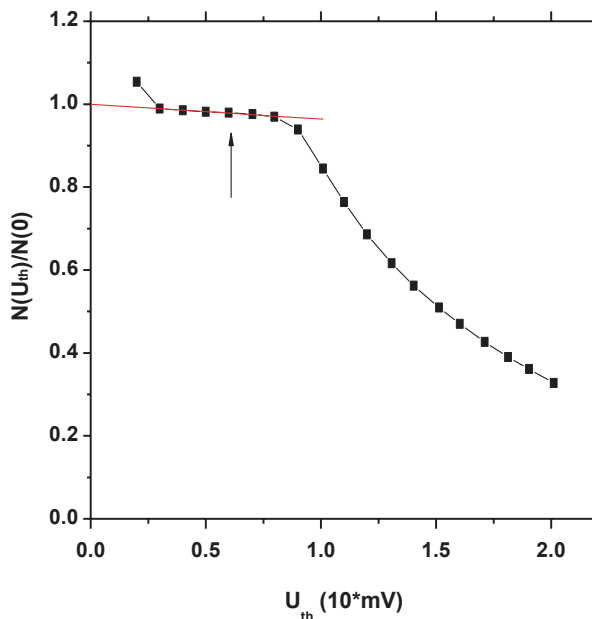
The pulse height (PH) distribution of FF was measured by integrating FF events above a given threshold of a constant fraction discriminator (CFD) [21]. This dependence is shown in Fig. 2.2. The efficiency of the FF counting at the applied threshold has been determined to be 0.98 ± 0.01. It was estimated by extrapolating the plateau region in Fig. 2.2 to zero threshold. The time resolution, estimated on the basis of the width of the prompt fission gamma-rays, measured with a small Pilot U scintillator, was ~ 1 ns at full width of half maximum (FWHM).

2.1.2 Neutron Spectroscopy by TOF Method

Since beginning of 1970s, practically all PFNS were measured by TOF method. For its realization, we should have "start" and "stop" pulses. The stop signal as a rule generated by FF or from accelerator operating in "pulse mode." The start signal is the task of ND. Several types of NDs used for spectroscopy of PFN are: ^{6}Li-glass scintillator, antracene ($E_n < 3$ MeV), crystal (stilbene) or liquid organic scintillators for neutrons with energy from ~ 0.5 till 20 MeV. After subtraction of neutron background, and the transformation to energy scale taking into account relativistic formulas, the investigated spectrum $S(E)$ is connected with experimental distribution $N(E)$ by Eq. (2.1). If the PFNS from fissile target A is measuring relative to ^{252}Cf standard we have two similar equations:

$$N_x(E) = Y_x \cdot S_x(E) \frac{v_x}{4\pi} \Omega \cdot \varepsilon(E) \cdot \alpha_1(E) \ldots \alpha_n(E), \qquad (2.1)$$
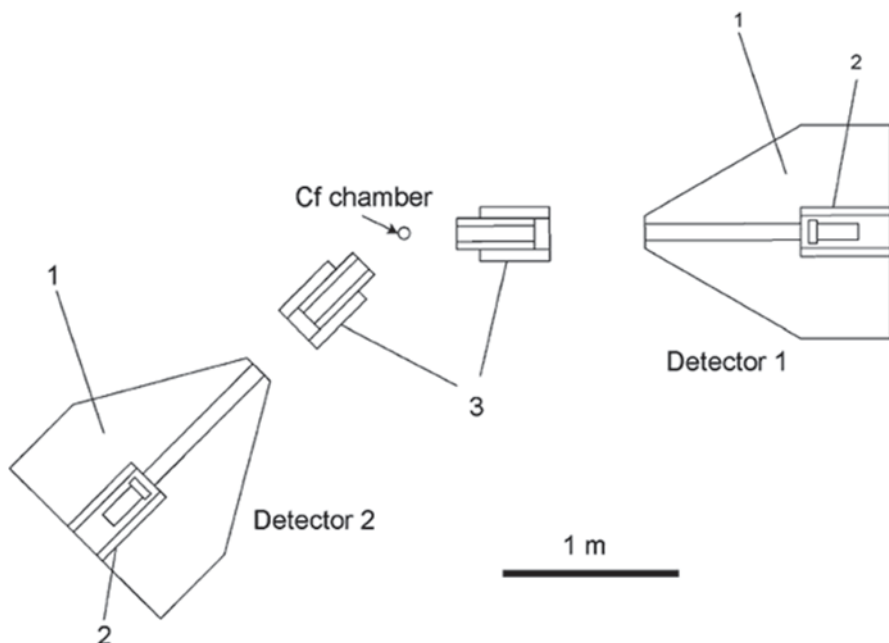
Fig. 2.3 Experimental setup for two detectors. *1* lithium carbonate; *2* lead; *3* Cu cylinders

where $x=A$,Cf, Y—yield of the FFs measured during the run, ν—neutron multiplicity, Ω—detector solid angle, $\varepsilon(E)$—detector efficiency, $\alpha_i(E)$—any necessary corrections for: neutron scattering in the chamber materials, time-resolution and bin corrections, and others possible factor which may destroy PFNS.

The experimental spectra taken with Cf—$N_{Cf}(E)$ may be used for detector efficiency estimation. The comparison of this result with calculated data gives an additional verification of the experimental method. In reality, the A spectrum $S_A(E)$ may be estimated directly from the ratio $S_A(E)/S_{Cf}(E)$. So, the knowledge of the detector efficiency is not a crucial factor, more important is the correction due to multiple scattering. The FF yields, Y_x, were measured during the same experimental runs (if both layer A and Cf are placed in the same counter); therefore, in some experiments data are normalized to the neutron multiplicity. So, both values ν_U and ν_{Cf} are known with high accuracy, and comparison with our experimental result may be a good test, also. In case of "solid sample" experiment as a rule only relative PFNS shape is investigation (Y is unknown).

The following discussion will be based on the experimental setup which was used in JRC-IRMM [21]. In this work, the properties of several organic NE213 equivalent NDs, namely three SCIONIX LS301 ($\varnothing=10$ cm; $h=5$ cm) and the BICRON BC501A ($\varnothing=10$ cm; $h=2.5$ cm) were investigated. In all cases, the scintillators were coupled to XP4312 photomultiplier (PM) tubes. During the measurement the detectors were placed in massive shieldings. Up to three detectors were used simultaneously. The experimental setup for two detectors is shown in Fig. 2.3.
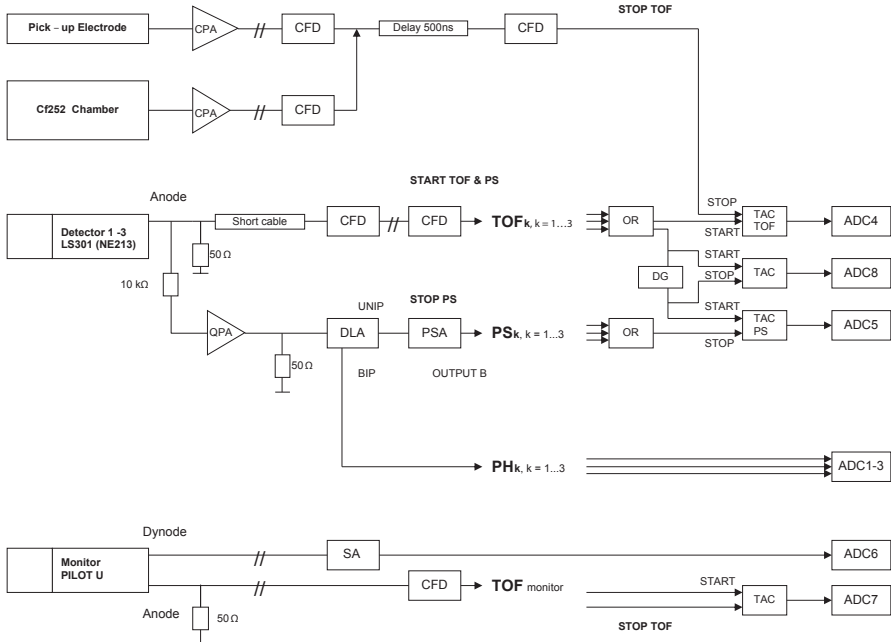
Fig. 2.4 Block-diagram of the electronic setup. *CPA* current sensitive preamplifier, *CFD* constant fraction discriminator, *QPA* charge sensitive preamplifier, *TOF* time-of-flight, *PS* pulse shape, *TAC* time-to-amplitude converter, *ADC* analog-to-digital convertor, *PSA* pulse shape analyzer, *DLA* delay line amplifier, *BIP* bipolar output, *SA* spectroscopic amplifier, *UNIP* unipolar, *PH* pulse height

The block-diagram of the electronic setup for three detectors is shown in Fig. 2.4. The anode signal of the PM tube was used for event timing and for neutron–gamma discrimination. A small part of the anode current (1/400) was transmitted to the QPA. The integrated pulse was fed over a long cable to a delay line amplifier (ORTEC 460) and its unipolar (UNIP) output signal was connected to a pulse shape analyzer (PSA, ORTEC 552). The "B outputs" of the three PSA have been linked by an OR module and via a time-to-amplitude converter (TAC PS) to the analog-to-digital convertor (ADC 5) for pulse shape (PS) measurements. The bipolar output (BIP) signal was directly connected to ADCs 1, 2, 3, for PH measurements. These ADCs were used for detector identification. The main part of the anode pulse was transmitted through a rather short cable (~1–2 m) to a CFD. After the OR-unit these signals were used to provide a "start" pulse for the TOF (TAC TOF) and pulse shape measurements (TAC PS). The "B output" of the PSA is delayed by about 1 ms relative to the CFD output. Therefore, an additional delay of about 500 ns (DG—delay generator) was used to reduce the dynamic range of the PS. The real delay was measured for each event (ADC 8) and was applied in the offline analysis to remove the time drift of this device. A small Pilot U detector was used as a time resolution monitor. The dynode output was connected directly to the spectroscopic amplifier (SA) and was applied for PH analysis (ADC 6). The anode output after the CFD

was connected to the start input of the TAC and ADC 7 for the TOF measurement. The "stop" signal for the TOF measurement was generated from the Cf-IC (current sensitive preamplifier, CPA) or from the pick-up electrode of the Van de Graaff accelerator as a pulsed source of mono-energetic neutrons using the same electronic equipment. The signal was delayed with a long cable for 500 ns to detect the "parent" pulse for any ND pulse.

The data were collected in list mode with the data acquisition software. During offline analysis the data may be sorted into different combinations to provide the best way for the estimation of the detector parameters: TOF versus PH, PS versus PH, and PS versus TOF. The original data were collected utilizing 8192 channels for each ADC. The TOF channel width was 0.1173 ns.

2.1.3   Time-Correlated Background

Fission events counted with any detector have random time distribution. One may define the following possibilities correlation between FF and ND events.

Real coincidences In this case, the ND and chamber pulses belong to the same fission event.

Time-Independent Background—$S_{tib}(i)$ The natural γ-ray background or gamma-rays from the β-decay of FF are counted by the ND and this pulse coincides with the FF pulse. These events have an exponential time-dependence due to the random nature of the fission process. This background may be calculated with Eq. (2.2):

$$S_{tib}(i) = N_0 \cdot \exp(-i\tau A_f), \quad N_0 = \frac{\sum_{i=i_1}^{i=i_2} N_i \cdot \exp(i\tau A_f)}{i_2 - i_1 + 1}, \tag{2.2}$$

where N_i is the measured TOF distribution versus the channel number i; i_2, i_1 are the channel numbers at the right side of the prompt gamma-ray peak used for the calculation of the time-independent background N_0, A_f is the FF count rate, and τ is the channel width.

Random coincidences—$S_{tcb}(i)$ (time-correlated background) In this case, the ND and chamber pulses belong to a different fission event, but they conserve a time correlation due to the time dependence of the neutron and γ-rays from FFs. This background may be calculated according to:

$$S_{tcb}(i) = \tau \cdot A_f \cdot \exp(i\tau A_f) \sum_{j=i+1}^{i_{max}} N_i^{cor}, \tag{2.3}$$

where N_i^{cor} is the TOF spectrum after subtraction of $S_{tib}(i)$. All background components are given in Fig. 2.5.

Fig. 2.5 TOF spectrum after
(n-γ) discrimination and
background components for
the ^{252}Cf source. The channel
width is 0.485 ns. *Lines* show
the background components:
time-independent back-
ground (*dotted*) and random
coincidence (*dashed*). *The
full* line is the sum of both
background components
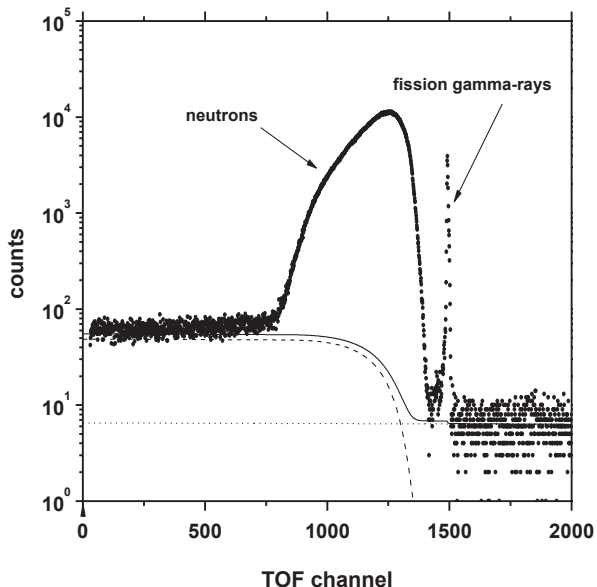
Finally, the net effect may be found according to:

$$S_{ef}(i) = \exp(i^{\tau} A_f) \cdot \left[N_i^{cor} - S_{tcb}(i) \right]. \tag{2.4}$$

All spectra and corrections should be calculated in time scale. The time cor-
related background in [21] was rather small due to the low activity of the ^{252}Cf
($A_f < 4 \cdot 10^4$ ff/s). So, it was smaller than 5 % at an energy of about 0.5 MeV.

2.1.4 Time Shift in Neutron Detector

The time reference in the TOF spectrum is indicated by the prompt γ-peak. This
time reference can also be used to observe a time shift depending on the PH. Mainly
this effect is connected with nonideal operation of the CFD.

The effect has been investigated with the present setup. The data were collected
in a matrix PH versus TOF of 128×2048 channels. In the first step, the centers of
gravity for prompt γ-ray events have been calculated for each PH bin. This peak
position information was used to compensate the time shift. Of course, we assumed
that the main contribution in the time shift appeared due to the CFD operation which
is common for protons and gamma-rays. In Fig. 2.6, the position of the prompt γ-ray
peak is shown before and after the time shift correction. The residual difference may
be explained due to the finite width of the TOF channel (0.1173 ns).

Fig. 2.6 The position of the
prompt γ-rays before (*open*)
and after time reference cor-
rection (*full squares*)
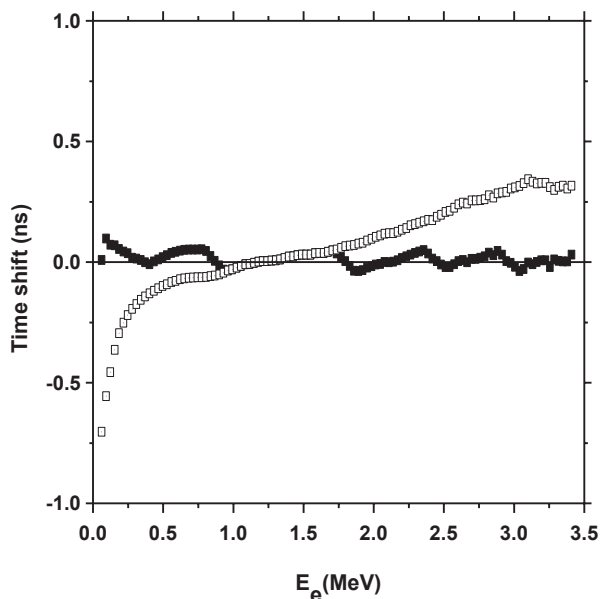
The specific effect may appear due to the fact that the ND pulses have a non-
"standard" shape (the beginning part of the ND pulse may be distorted by multiple
scattering in the scintillator). However, this effect was not investigated in details.

2.1.5 Neutron-Gamma Discrimination and its Influence on Result

The ND on the basis of NE213 liquid, and crystal scitillators like stilbene, antracene
have very useful properties—PS (contribution fast and slow components) depends
on particle. This fact allows us to reduce gamma rays' background very much. In the
same time it may provide an additional distortion effect.

The difference between PS for protons and electrons at low proton energy,
<1 MeV, reduced very much due to small amount of emitted photons and big fluc-
tuation. The example is shown for two amplitudes of signal ~0.2 MeVee and 0.4
MeVee of electron energies (Fig. 2.7). At low energies, the PS distributions are
overlapping, and as a result some part of protons' events (neutrons) may be lost.

There is another factor—multiple scattering inside scintillator, which may
change the PS for neutron counting. It has already been discussed in Sect. 2.1.4.

For example, the detector was exposed with 5 MeV neutron. After first scatter-
ing, it produced ~4 MeV protons and residual ~1 MeV neutron may give new pulse
inside scintillator. If the scintillator has average size ~10 cm, the second pulse will
be shifted relative to first one on ~7 ns. It is not clear how this PS will be treated
by analyzing device. These events may be removed from counting procedure and